Maintaining Rice Production while Mitigating Methane and Nitrous Oxide Emissions from Paddy Fields in China:
Evaluating Tradeoffs by Using Coupled Agricultural Systems Models

Zhan Tian[1], Yilong Niu[1, 2], Dongli Fan[2], Laixiang Sun[3, 4, 5], Gunther Ficsher[4], Honglin Zhong[3], Jia Deng[6], Francesco N. Tubiello[7]

1. Shanghai Climate Center, Shanghai Key Laboratory of Meteorology and Health, Shanghai Meteorological Service, Shanghai 200030, China
2. Shanghai Institute of Technology, Shanghai, 201418
3. Department of Geographical Sciences, University of Maryland, College Park, MD 20742, USA
4. International Institute for Applied Systems Analysis (IIASA), A-2361 Laxenburg, Austria
5. School of Finance & Management, SOAS, University of London, London WC1H 0XG, UK
6. Earth Systems Research Center, Institute for the Study of Earth, Oceans, and Space, University of New Hampshire Durham, NH 03824, USA
7. Statistics Division, Food and Agriculture Organization of the United Nations (FAO), Rome, Italy

Correspondence to: Dongli FAN, E-mail: fandl@sit.edu.cn; or Laixiang Sun, Email: LSun123@umd.edu, Tel: +1-301-405-8131, Fax: +1-301-314-9299.

ABSTRACT

China is the largest rice producing and consuming country in the world, accounting for more than 25% of global production and consumption. Rice cultivation is also one of the main sources of anthropogenic methane (CH_4) and nitrous oxide (N_2O) emissions. The challenge of maintaining food security while reducing greenhouse gas emissions is an important tradeoff issue for both scientists and policy makers. A systematical evaluation of tradeoffs requires attention across spatial scales and over time in order to characterize the complex interactions across agricultural systems components. We couple three well-known models that capture different key agricultural processes in order to improve the tradeoff analysis. These models are the DNDC biogeochemical model of soil denitrification-decomposition processes, the DSSAT crop growth and development model for decision support and agro-technology analysis, and the regional AEZ crop productivity assessment tool based on agro-ecological analysis. The calibration of eco-physiological parameters and model evaluation used the phenology and management records of 1981-2010 at nine agro-meteorological stations spanning the major rice producing regions of China. The eco-physiological parameters were calibrated with the GLUE optimization algorithms of DSSAT and then converted to the counterparts of DNDC. The upscaling of DNDC was carried out within each cropping zone as classified by AEZ. The emissions of CH_4 and N_2O associated with rice production under different management scenarios were simulated with the DNDC at each site and also each 10×10 km grid-cell across each cropping zone. Our results indicate that it is feasible to maintain rice yields while reducing CH_4 and N_2O emissions through careful management changes. Our simulations indicated that a reduction of fertilizer applications by 5-35% and the introduction of midseason drainage across the nine study sites resulted in reduced CH_4 emission by 17-40% and N_2O emission by 12-60%, without negative consequences on rice yield.

KEY WORDS: Climate change; agricultural CH_4 and N_2O emissions; rice yield; model coupling; mitigation tradeoffs; China

INTRODUCTION

Climate change characterized by global warming has already had observable impact on the ecological system and human society (Alley et al., 2003). The historical records show that from 1901 to 2012, the global mean surface temperature increased by 0.89℃. This warming trend is expected to continue in the forthcoming decades and would impose even more significant impact on ecosystem and human society (IPCC, 2013). The main cause of current global warming is the anthropogenic emission of greenhouse gases (GHGs), which has led to their increased concentration in the atmosphere. Modern intensive farming, which heavily depends on chemical fertilizer application and irrigation, is the single largest source of methane (CH_4) and nitrous oxide (N_2O) emissions (IPCC, 2014; FAO, 2016). Meanwhile, a warmer climate accompanied by modified water regimes exerts impact on farming practices and consequently on crop productivity (Verburg et al., 2000; IPCC, 2014). Since the global warming potential of CH_4 and N_2O is 25 and 298 times higher than CO_2, respectively (IPCC, 2013), it is well recognized that a focus on reducing CH_4 or N_2O emissions may be an effective climate change mitigation strategy.

Our ability to pick these "low-hanging fruits" may however be constrained by the existence of multiple, conflicting objectives. Rice paddy cultivation in China represents a significant example to this end. On the one hand, China is the major producer and consumer of rice in the world and maintaining self-sufficiency in rice is extremely important for the country (FAOSTAT 2016). On the other, China's rice production generates significant environmental pressure, as it depends on large-scale basin irrigation and large amounts of fertilizers applications (Miao et al., 2011). Such practices have resulted in significant emissions of CH_4 and N_2O to the atmosphere, as well as damages to soil and water systems. Using IPCC guidelines for GHG inventories (IPCC, 2006), the emissions of CH_4 from Chinese paddy fields were estimated at 7.41 Tg (1 Tg = 10^{12} g) CH_4-C in 2000, which is well over 150 Tg CO_2eq, accounting for about 29% of world total CH_4 emission from rice in that year (Yan et al., 2009). These emissions levels were maintained throughout the last decade (FAOSTAT, 2016). At the same time, N_2O emissions from Chinese paddy fields were estimated at 0.036 Tg N_2O-N in 2007 (Gao et al. 2011), corresponding to roughly 30% of the total N_2O-N emissions from Chinese agriculture (FAOSTAT, 2016).

In the rice cultivation system, rice grain and greenhouse gas are joint products from paddy fields cultivation and there is a complex relationship between rice growing and GHG emissions. For example, CH_4 production is influenced by substrate concentrations, which are

102   influenced by plant root activities. Plant growth dynamic also influences soil mineral N

103   through crop N uptake, therefore indirectly affecting N_2O emission. This complexity has

104   attracted significant research attention and various GHG mitigation measures have been

105   tested using field experiments at paddy sites. For example, Dong et al. (2011) highlighted the

106   tradeoff relationship between CH_4 and N_2O emissions, finding that an increasing application

107   of nitrogen fertilizer will mitigate CH_4 emission with reference to no fertilization, but

108   increase N_2O emissions at the same time. Itoh et al. (2011) found that employing midseason

109   drainage as a water management technique in rice fields reduced the combined climate

110   forcing of CH_4 and N_2O in comparison with basin irrigation. Based on experimental evidence,

111   Johnson-Beebout et al. (2009) concluded that simultaneous minimization of both CH_4 and

112   N_2O emission could not be maintained in rice soils, but that appropriate water and residue

113   management could nonetheless reduce greenhouse gas emissions. Wu et al. (2008) showed

114   that employing conservation tillage methods, especially no-tillage, mitigated GHG emission

115   from rice fields by about 15%. However, it is difficult to extrapolate these field-based results

116   to large regional scales, because of high inherent variability over space and time. Such

117   variability may instead be addressed by agricultural systems models that, while capturing the

118   fundamental soil crop atmosphere dynamics highlighted by field experiments, can be used to

119   further estimate the regional variability of associated emissions as a function of the wide

120   range of soil, water and climatic parameters that exists over large scales (Jones et al., 2016).

121   The DeNitrification-DeComposition (DNDC) model is one of the most widely accepted

122   biogeochemistry process-based models in the world (Wang and Chen, 2012; Gilhespy et al.,

123   2014). The model has been evaluated against observations worldwide (e.g., Beheydt et al.,

124   2007; Giltrap et al., 2010; Gilhespy et al., 2014). The development of a GIS coupled to high-

125   resolution soil maps in recent versions of this model, allows DNDC to also estimate GHG

126   emissions at regional and national levels, in support of national inventories and including the

127   impacts of rice rotations (e.g., Gilhespy et al., 2014; Zhang et al. 2016; Li et al. 2005; Chen et

128   al. 2016).

129   With the GIS application, an array of weather and soil data could be employed to

130   support DNDC model-based regional simulations. However, two limitations currently

131   undermine such simulations. First, the phenological and physiological parameters as the key

132   input of DNDC are typically calibrated with the subjective optimization method (McCuen,

133   2003), meaning that parameter values are manually adjusted based on the modeler's

134   subjective knowledge of the parameter, model, and data (Wang and Chen, 2012). A

135   consequence of this limitation is that the default cultivar parameter values in DNDC

136 characterize only one rice cultivar for all of China, thus failing to represent the richness and
137 regional diversity of cultivars that exists in this country. Second, as highlighted in Zhang et al.
138 (2016), most DNDC studies were conducted at the county level in the case of China or at
139 large spatial simulation units, with a resolution about $0.5° \times 0.5°$ (e.g., Li, 2000; Pathak et al.,
140 2005; Tang et al., 2006; Gao et al., 2014). This coarseness does not allow to properly capture
141 the impacts of soil heterogeneity and the associated management measures within a county or
142 a large spatial unit, resulting in poor spatial performance of the simulation models.

143 To overcome the above weaknesses of DNDC and to more accurately evaluate the
144 tradeoffs between maintaining the current level of rice production and reducing GHG
145 emissions from farming activities, we coupled three state-of-the-art agricultural systems
146 models in order to capitalize on their individual comparative advantages. They are the
147 biogeochemistry process-focused DNDC model, the crop growing process-focused model –
148 Decision Support System for Agro-technology Transfer (DSSAT) (Jones et al. 2003), and the
149 Agro-Ecological Zone (AEZ) model (Fischer et al. 2012), a widely used regional crop
150 productivity assessment tool. The two crop simulation models (DSSAT and AEZ) are
151 designed to assess the impacts of multiple climate factors on crop growth and grain yield.
152 They are widely employed in climate impact studies (Challinor et al., 2014; Thorp et al.,
153 2008; Seidl et al., 2001). We investigated how such coupling can improve the spatial
154 performance of DNDC for the case of paddy rice production in China. Our parameters
155 calibration and model evaluation used the observed phenology and management records at
156 nine representative agro-meteorological stations, spanning the major rice producing regions
157 of China. We first calibrated eco-physiological (cultivar) parameters for rice growth using the
158 Generalized Likelihood Uncertainty Estimation (GLUE) algorithm provided by DSSAT,
159 which uses Monte Carlo sampling from prior distributions of the coefficients and a Gaussian
160 likelihood function to determine the best cultivar coefficients, based on the observation data.
161 We then followed a procedure as presented in Section 2.4.2 to convert these eco-
162 physiological cultivar parameters into DNDC required parameters. In this way, we enriched
163 the value set of cultivar parameters of the DNDC model, which is essential for meaningfully
164 upscaling, via the assistance of AEZ, the DNDC runs to the rice cropping zones of China.
165 With such coupling between the three models, we evaluated rice yield levels and the
166 corresponding CH_4 and N_2O emissions under different management scenarios, at a resolution
167 of 10×10 km, seeking to highlight those water and fertilizer management solutions that could
168 lead to significant reduction of CH_4 and N_2O emissions without causing reductions in rice

169   production.

170

171   **2. MATERIALS AND METHODS**

172   **2.1 The study sites**

173   We selected nine agro-meteorological observation stations based on the following

174   criteria from the original hardcopy records filed in the Data Center of China Meteorological

175   Administration: (1) each station represents a typical cropping system for rice cultivation in

176   China; (2) they differ in terms of geographic and climatologic characteristics; (3) each station

177   has complete records of crop phenology for more than 20 years over the period of 1981-2010;

178   and (4) each station has complete records of crop management for more than 5 years over the

179   period of 1981-2010. These records include the ID, name and location (latitude and longitude)

180   of each station; date of each major phenological stages (sowing, flowering, maturity, etc.);

181   yield and yield components (grain weight, grain number per tiller, tiller number per plant,

182   etc.); date, type and quantity of fertilizer application; and irrigation methods and dates. These

183   crop phenology and management data are critical for simulating crop growing and

184   quantifying CH_4 and N_2O emission from crop fields. Table 1 and Figure 1 report names,

185   locations, and geographical features of these nine stations.

186
187   (*Table 1 and Figure 1 are about here*)
188

189   **2.2 Input Datasets at the Grid-cell Level**

190   Observed daily weather data, including minimum and maximum air temperature, daily

191   sunshine hours, precipitation, relative humidity, and wind speed, for 1981-2010 at over 700

192   observation stations nationwide were provided by the Data Center of China Meteorological

193   Administration. Because all three models need solar radiation data, we employed the

194   empirical global radiation model to calculate daily radiation levels (Pohlert, 2004). These

195   point-based data are imported to ArcGIS together with the coordinates and then interpolated

196   into 10 km spatial resolution raster data.

197   The Harmonized World Soil Database (HWSD, cf. FAO/IIASA/ISRIC/ISSCAS/JRC,

198   2009) provides reliable and harmonized soil information at the grid cell level for the world,

199   with a spatial resolution of 1 km × 1 km for China. The soil is divided into topsoil (0–30 cm)

200   and subsoil (30–100 cm). Each grid cell in the database is linked to commonly used soil

201   parameters. Most of the minimum soil properties required by the DSSAT and DNDC models

202   can be extracted directly from the HWSD soil database. For the missing soil surface albedo,

203 we used the soil color from the World Inventory of Soil Emission Potentials (WISE) soil
204 database (Batjes, 2009) and determined the soil surface albedo with the standard given by
205 Ritchie et al. (1989). We calculated other missing soil properties with extracted soil properties
206 and procedures provided in the DSSAT literature (Gijsman et al., 2002, 2007), such as USDA
207 curve number (Lane, 1982) and drainage rate, root growth factor, upper and lower limit of
208 plant extractable soil water.

209 The map of paddy fields is extracted from the National Land Cover database (100 m ×
210 100 m) provided by the Institute of Geographical Sciences and Natural Resource Research
211 (IGSNRR) of the Chinese Academy of Sciences. The reference year for the map is 2000. This
212 land cover database is produced from visual interpretation of Landsat ETM/ETM+ satellite
213 images and grouped into ten categories. Paddy field is one of the major categories (Liu et al.,
214 2005).

215

216 **2.3 Agricultural Systems Models**

217 **2.3.1 The DNDC model**

218 The DeNitrification-DeComposition (DNDC) model simulates soil carbon (C) and
219 nitrogen (N) biogeochemical processes in crop growth cycle. It was originally developed for
220 simulating C sequestration and emissions of greenhouse gases from agricultural soils in the
221 USA (Li et al., 1992; Li et al., 1994). During the last 25 years, the DNDC model has been
222 developed to simulate C and N transformations in different ecosystems, such as forest,
223 wetlands, pasture, and livestock farms. It has incorporated a relatively complete suite of
224 biophysical and biogeochemical processes, which enables it to compute the complex
225 transport and transformations of C and N in terrestrial ecosystems under both aerobic and
226 anaerobic conditions (Gilhespy et al., 2014; Li 2007).

227 DNDC is comprised of six interacting sub-models: soil climate, plant growth,
228 decomposition, nitrification, denitrification, and fermentation. The soil climate, plant growth,
229 and decomposition sub-models convert the primary drivers into soil environmental factors.
230 The nitrification, denitrification, and fermentation sub-models simulate C and N
231 transformations that are mediated by soil microbes and controlled by soil environmental
232 factors (Li 2000; Li et al., 2012). In DNDC, crop biomass and yield are simulated at daily
233 time steps by considering the effects of several environmental factors on plant growth,
234 including radiation, air temperature, soil moisture, and N availability. Methane flux is
235 predicted by modeling CH_4 production, oxidation, and transport processes. CH_4 production is
236 simulated by calculating substrate concentrations (i.e., electron donors and acceptors)

resulting from decomposition of SOC (soil organic carbon) as well as plant root activities including exudation and respiration, and then by simulating a series of reductive reactions between electron donors (i.e., H_2 and dissolved organic carbon) and acceptors (i.e., NO_3^-, Mn^{4+}, Fe^{3+}, SO_4^{2-}, and CO_2). Redox potential, temperature, pH, along with the concentrations of electron donors and acceptors are the major factors controlling the rates of CH_4 production and oxidation. DNDC simulates CH_4 transport via three pathways, including plant-mediated transport, ebullition, and diffusion (Fumoto et al., 2008; Zhang et al., 2002). N_2O is simulated as a by-product of nitrification and denitrification. As microbial-mediated processes, both nitrification and denitrification are subject to complex regulation of numerous environmental factors, such as concentrations of mineral N, availability of dissolvable organic carbon (DOC), redox potential, and temperature in DNDC (Li, 2000). Farming management practices, such as synthetic fertilizer application, manure use and irrigation, have been parameterized to regulate the soil N dynamics, DOC availability, and/or soil environments, and therefore regulate N_2O emissions from soils. In this research, we use the latest version of DNDC (DNDC 95).

2.3.2 The DSSAT model

The Decision Support System for Agro-technology Transfer (DSSAT) model (Jones et al., 2003; Hoogenboom et al. 2010) is a popularly-employed model for simulating crop growing dynamics (Challinor et al., 2014). The core of the DSSAT system consists of 17 crop simulation models. This research employs the Crop Environment Resource Synthesis (CERES) model, which simulates cereal crops such as wheat, rice and maize. The CERES model calculates daily phenological development (i.e., vegetative growth, flowering, grain growth, maturity and senescence phases) and biomass production in response to environmental (soil and climate) and management (crop variety, planting conditions, N fertilization, and irrigation) factors.

The crop cultivar parameters, which are named genetic coefficients in DSSAT, quantitatively describe how a particular genotype of a cultivar responds to environmental factors (Penning de Vries et al., 1992), thus enabling the integration of genetic information on physiological traits into crop growth models. Each crop in the model has a specific set of parameters, values of which characterizes the genetic information of different cultivars. In the CERES-rice model, 8 parameters are essential for describing the genetic information of different rice cultivars (Prasada Rao, 2008, Table 14.1). Because each station belongs to a specific cropping zone/cropping system for rice cultivation in China as we presented in

Section 2.1, we have nine cultivars, each at one station. We employ the DSSAT-provided Generalized Likelihood Uncertainty Estimation (GLUE) method (He et al., 2010) to estimate the parameter values of the given cultivar. GLUE is a Bayesian estimation method. GLUE uses Monte Carlo sampling from prior distributions of the coefficients and a Gaussian likelihood function to determine the best coefficients based on the observation data. It has been widely used in crop and hydrological modeling (Blasone et al. 2008; He et al., 2010; Wang et al. 2015). The technical details of the GLUE estimation and a part of the estimation results were published in Tian et al. (2014). The procedure on translating DSSAT's genetic coefficients into the format of DNDC's cultivar parameters will be presented in sub-section 2.4.2.

2.3.3 The AEZ model

In contrast to the process-based crop growth model like DSSAT, the Agro-Ecological Zone (AEZ) model, which was jointly developed by the International Institute for Applied Systems Analysis (IIASA) and the Food and Agricultural Organization (FAO) of the United Nations, is a regional scale model to simulate land resource and crop production potential (Fischer et al., 2012). AEZ provides a standardized crop-modeling and environmental matching procedure, which classify a region into cropping zones based on climate, soil, and terrain characteristics relevant to specific crop production, and identify crop-specific limitations of prevailing agro-ecological resources under assumed levels of inputs and management conditions. This procedure in AEZ makes it well suited for crop suitability, zoning, and productivity assessments at regional, national and global scales (cf., among others, FAO, 2007; Fischer et al., 2005; Gohari et al., 2013; Masutomi et al., 2009; Tian et al., 2012, 2014; Tubiello and Fischer, 2007). In each rice-cropping zone identified by the AEZ, we have one representative observation station (Fig. 1). We assume that the rice cultivar parameters we have calibrated at the representative station are applicable for DNDC simulations across grid cells within this rice cropping zone.

2.4 Implementation Procedure of Model Coupling

The flowchart for effectively linking DSSAT, AEZ, and DNDC models are presented in Fig. 2. As shown in Fig.2, the central purpose of the model coupling is for finding feasible ways to reconcile the two policy goals of maintaining rice production and mitigating methane (CH_4) and nitrous oxide (N_2O) emissions from paddy fields in China. The reconciliation would become more convincing if both rice production and the corresponding CH_4 and N_2O

emissions are outputs of one model, and the most suitable model for this purpose is the DNDC. However, despite that DNDC model has the designed comparative advantage in simulating biogeochemistry process during crop growing cycle and it is also capable of simulating crop growing process, its simulations are subject to the condition that the representative phenological and physiological parameters related to crop growth simulations with DNDC are available as the key input information (User's Guide for the DNDC Model, http://www.dndc.sr.unh.edu/model/GuideDNDC95.pdf). To produce such representative phenological and physiological input parameters for DNDC, DSSAT has clear comparative advantage because the DSSAT model is designed for simulating very detailed crop-growing process, including phenological details. The central steps for enriching the parameter value set of rice cultivars in the DNDC model and to enable the smooth up-scaling runs of DNDC within each rice-cropping zone of China's rice growing region are as follows. (1) calibrating rice genetic coefficients at the nine agro-meteorological stations using the DSSAT model and its GLUE algorithms; (2) converting the newly calibrated genetic coefficients into the format of DNDC; (3) reclassifying the cropping zones based on the spatial relationship between observed cropping practices at the nine stations and the two-digit classification of the AEZ cropping zones, so that each rice cropping zone has only one set of DNDC parameter values; and (4) simulating CH_4 and N_2O emissions under different scenarios using the DNDC model with the calibrated values of crop cultivar parameters remaining stable in each of the reclassified cropping zones, under the historical climate conditions from 1981 to 2010.

(*Figure 2 and Table 2 about here*)

2.4.1 Scenarios configuration

In order to find one or more feasible management methods which can meet the dual goal of maintaining the current level of rice production and reducing GHG emissions from the current emission level, we set up 4 management scenarios and simulate rice growing and GHG emission processes for a single rice growing season under each scenario.

The first one is the "Traditional Management" (TM) scenario, in which the application of chemical fertilization follows the existing practice and irrigation follows the current continuous flooding, with the timing and intensity as recoded in the observation data of the nine study sites.

Excessive application of nitrogenous fertilizer has been widely recognized as an important source of excessive N_2O emission from rice paddy fields, as discussed in the

339 introduction. We define a threshold/balanced fertilizer amount which guarantees the best

340 attainable yield with the minimum amount of necessary fertilizer application, meaning that an

341 application amount smaller than this threshold will lead to yield reduction even under ideal

342 weather and water management conditions, and an application amount larger than this

343 threshold will not lead to an increase in yield. In order to find this threshold, the maximum

344 amount of the observed fertilizer application at each station was employed as the starting

345 point. Then we ran DNDC simulations stepwise and at each step we cut down this maximum

346 amount by 5% and check its impact on the best attainable yield. In this way we found the

347 ratio of the threshold/balanced fertilizer amount to the real maximum application amount at

348 each of the 9 stations. We call this ratio the 'balanced fertilizer ratio' (Table 2). Consistent

349 with the acknowledgement in the literature, excessive application is present in all nine

350 stations, being 5-35% higher than the requirement for supporting the best attainable yield.

351 While the SCCD and JXNC sites reported a moderate extent of excessive fertilizer

352 application, all other sites showed significant room for reducing fertilizer application amount.

353 The above search procedure leads to the establishment of the second scenario, which consists

354 of the balanced fertilizer application and continuous flooding irrigation method. We call it the

355 "Balanced Fertilizer" (BF) scenario.

356 With the development of new crop management and cultivar breeding technology,

357 increasing number of farmers are using the midseason field drying method to replace the

358 traditional basin irrigation method, which could mitigate CH_4 emission effectively. We name

359 this scenario "Midseason Drainage" (MD), in which the application of fertilizer is as the

360 observed, but irrigation management takes the midseason field drying method.

361 The forth scenario, we call it "Comprehensive Mitigation" (CM), combines the balanced

362 fertilizer application and the midseason field drying irrigation method. Because changes in

363 water management method will affect nitrification and denitrification processes, under the

364 MD and CM scenarios, the balanced fertilizer application amount at JXNC decreases from 90%

365 to 80% and at LNTT increases from 80% to 95% (Table 2, BFR-1 and BFR-2).

366

2.4.2 Calibration of cultivar parameters and DNDC validation

368 Key rice cultivar parameters related to the simulation of crop growth and GHG

369 emissions in DNDC include maximum biomass and C:N ratio of grain, leaf, stem and root,

370 respectively; optimum rice growing temperature; and the required accumulative degree days

371 (TDD) from sowing to maturity. In order to improve the information on rice cultivars in the

372 DNDC model, we first calculate the maximum grain biomass based on the yield records at

373   each observation site. We determine the best attainable yield based on the maximum value of

374   the multi-year yield components records, which includes the maximum grain number per

375   tiller and the corresponding grain weight, maximum tiller number per plant and the optimum

376   plant density. This way of determining the maximum grain biomass is in line with the

377   corresponding requirements in the DNDC setting. It also guarantees that the ways we find for

378   reducing CH_4 and N_2O emission are able to maintain the best attainable yield. Second, we

379   employ the GLUE module in the DSSAT model to calibrate the rice genetic coefficients by

380   targeting at the maximum grain biomass at each station. We used the outputs of DSSAT

381   model calibrated to calculate, for each site, the maximum biomass and the C:N ratio for each

382   part of the rice plant, and also the harvest index (HI). In the calculation of the C:N ratio, we

383   also take reference from the relevant information in the AEZ database to justify the range of

384   our calculations. Third, optimum temperature for rice growing is translated from reference

385   temperature in AEZ directly and the TDD is calculated based on the daily weather data during

386   each rice growing season over the period of 1981-2010. Table 3 reports the results of the

387   above calibration.

388

389   (*Tables 3-5 about here*)

390

391   We then ran the DNDC model using the newly calibrated cultivar parameter values

392   (Table 3), and validated the model by comparing the simulations against the observed best

393   attainable yield at the site level. The ideal field management practices are used to ensure that

394   the growing process is free from water and nitrogen stress, and only influenced by weather

395   and soil. We report both the ranges of simulated yields and the Relative Absolute Error

396   (RAE), as presented in Eq. (1), to evaluate the consistency between the observed and the

397   simulated values.

398

399   $$\text{RAE} = \frac{|\text{Obs} - \text{Simu}|}{\text{Obs}} \times 100\% , \qquad (1)$$

400

401   where "obs" refers to the observed value and "simu" the result of DNDC model simulation at

402   the give site. Because the focus of DNDC is on the interactions between the C and N

403   biogeochemical cycles and the primary ecological drivers in the cropping process, rather than

404   on simulating the detailed crop growing process, the major phenology information such as

405   plating and maturity days are the input of DNDC. This means that the performance

406   evaluation of DNDC should be based on the comparison between observed and simulated

407   yield and emissions.

408   Table 4 reports the observed best attainable yield, the minimum, mean, and maximum of

409   the simulated yields, and the average RAE at the nine stations for the period of 1981-2010. It

410   shows that while at 6 of the 9 stations, the observed attainable yield lies within the

411   uncertainty range of the simulated yields, the observed yield at JLYJ is 119 kg higher (with an

412   average RAE at 4.69%) than the simulated maximum and that at SDLY and GDGZ is 313 kg

413   (average RAE 7.72%) and 290 kg (average RAE 8.13%) lower than the simulated minimum,

414   respectively. Given that the gap between the observed yield and the nearest border value of

415   the simulated yield is less than 5% at these 3 stations, we can accept that that the simulated

416   attainable yield matches the observed best attainable yield relatively well. This means that the

417   DNDC model with our enriched value set of cultivar parameters is able to simulate rice

418   production level with relatively good accuracy at each of the nine stations.

419   We do not directly test the DNDC simulations of CH_4 and N_2O emissions against the

420   corresponding field records because there is no observations on CH_4 and N_2O emissions at

421   the nine stations. Instead, we employed the experiment records at the Nanjing station

422   presented in Cai (1997) to validate the performance of the updated DNDC model. The same

423   experiment records were also used to validate the DNDC model by Cai et al. (2003) and

424   Fumuto et al. (2008). We ran DNDC using daily weather, soil and farming management data

425   from Cai et al. (2003) and Fumuto et al. (2008) for the same experimental site. For cultivar

426   parameters, we used the calibrated values at Zhengjiang station, which is 65 km to the east of

427   Nanjing, on the same Yangtze River bank area. Table 5 compares our results with those of Cai

428   et al. (2003) and Fumuto et al. (2008). Our simulated yield is 7782.5 kg ha^{-1}, which is 12%

429   higher than the observed yield. In contrast, there is no yield validation results in Cai et al.

430   (2003) and Fumuto et al. (2008). Our CH_4 emission result of 77 kg C ha^{-1} is 1/3 higher than

431   the observed value but still 11 kg C ha^{-1} lower than the result of Fumuto et al. (2008). Our

432   N_2O emission result of 0.5 kg N ha^{-1} is much closer to the observed value than that of Cai et

433   al. (2003), which is 8 times higher than the observed value (Table 5).

434

435   **2.4.3 Reclassifying the rice cropping zones**

436   The cropping zone system defines the land use units in the AEZ by climate, soil and

437   terrain characteristics that are relevant to specific crop production. Cropping zones typically

438   represent the spatial distribution of crop cultivars in historical climate conditions (Tian et al.,

439   2012). In this research, the original two-digit rice cropping zone map of China as defined by

440   the AEZ model is employed. There are 14 rice cropping zones. For 9 of these 14 zones, we

441   directly established one-to-one correspondence between the zone and the station within the

13

442 zone. For each of the other 5 zones, the closest suitable cultivar station was chosen for the

443 zone. In this way, we reclassified the existing 14 zones into 9. The map of the reclassified rice

444 cropping zones, overlaid with the paddy field map of China in 2000, is presented in Figure 1.

445

446 (*Figures 3-7 about here*)

447

448 **3. RESULTS**

449 **3.1 The yield prediction performance of the original and updated DNDC models at the**

450 **regional level**

451 To show the improvement brought about by the cropping-zone specific enrichment of

452 rice cultivar parameters in terms of yield prediction at the regional level, we ran the DNDC

453 model with both the default and the enriched/updated value set of cultivar parameters across

454 paddy grid-cells for the best single season of rice. The two maps in Figures 3 show the results

455 on yield predictions from the DNDC model by using the default and enriched cultivar

456 parameter values, respectively. The predicted yields in both maps are presented as the

457 averages over 1981-2010. Figure 3-a shows that the single season rice yield is less than

458 4000kg ha^{-1} in a very large part of the middle and lower reaches of the Yangtze River Basin,

459 which is much lower than observations in this most important rice producing region of China.

460 In sharp contrast, this undesirable gap does not show up in Figure 3-b. In terms of the

461 cropping zone average, the predicted yields in Figure 3-b range from 7000kg ha^{-1} to 10000kg

462 ha^{-1}. These results validate our previous argument that using a single set of cultivar parameter

463 values cannot represent the richness of rice cultivars in a large rice producing country like

464 China and can result in poor prediction. This comparison confirms the necessity to calibrate

465 parameter values for more cultivars at multiple representative sites and to employ the

466 enriched parameter values to drive DNDC for the model applications over a large region.

467

468 **3.2. Site-level simulations**

469 The results of site-level simulations under the field management scenario of Traditional

470 Management (TM), Balanced Fertilizer (BF), Midseason Drainage (MD) and Comprehensive

471 Management (CM) are summarized into boxplots as presented in Figures 4 and 5. Figure 4

472 shows that these four field management methods are able to maintain the best attainable yield

473 under the condition without water and nitrogen stress. Formal *t*-tests also confirm this.

474 Figures 5-a and 5-b show the results on CH$_4$ and N$_2$O emissions, respectively. We first

475 focus on the comparison between TM and BF. The set of boxplots for CH$_4$ does not suggest

476　any significant change when moving from TM to BF. For example, at sites HNXY, JXNC and
477　LNTT, the mean CH_4 emission decreased by less than 1% when adopting the balanced
478　fertilizer technique, whereas at other six stations, CH_4 emission barely increased, in the range
479　0.11%-4.25%. In contrast, the set of boxplots for N_2O shows significant mitigation of N_2O
480　emissions at all stations in relation to the balanced application technique, with reductions in
481　emissions that ranged 10%-69% and an average reduction across all sites of 33%.

482　　　Second we compare the results between TM and MD. Figures 5-a and 5-b show that
483　employing midseason drainage irrigation method mitigated CH_4 emission significantly, with
484　a reduction ratio ranging 18%-39% and an average reduction across all sites by 25%.
485　However, this new water management measure did not yield consistent results in terms of
486　changes in N_2O emissions. At sites JSZJ and JXNC, N_2O emissions in fact increased by 24%
487　and 20%, respectively, whereas at the other 7 stations, N_2O emissions decreased in the range
488　4%-32%.

489　　　The third comparison is between TM and CM. Figures 5-a and 5-b show significant
490　reductions in both CH_4 (18%-40%) and N_2O emissions (12%-60%). The mitigation impacts
491　of this management scenario outperformed the other scenarios at all nine stations, as a result
492　of positive interactions between the water and fertilizer management measures tested. We
493　further carried out formal *t*-tests to check the level of statistical significance of the differences
494　between TM and CM at each site. The *t*-test results indicate that the reduction of CH_4
495　emission is consistently significant at the 1% level across all sites, and the reduction of N_2O
496　is statistically significant at the 5% (at LNTT site) or 1% level (at other 7 sites), with the only
497　exception at JXNC.

498
499　**3.3 Regional-level simulations**

500　　　We extended the simulations of comprehensive mitigation (CM) scenario to the paddy
501　grid-cells in each of the 9 re-classified rice cropping zone to quantify the regional effect of
502　the comprehensive mitigation measure. Figure 6 shows the changes in the predicted yields
503　under the CM scenario versus TM scenario at the grid-cell level. It shows that the CM
504　measure resulted in yield increases in China's major rice producing regions – the Sichuan
505　Basin and the middle and lower reaches of the Yangtze River Basin; yield losses of 5%-10%
506　in parts of Northeast China, Ningxia's Hetao irrigation district and the northeast part of
507　Jiangsu province; and no changes or slight yield losses of less than 2% in other areas. At the
508　same time, the CM measure led to significant reductions in CH_4 and N_2O emissions (Figure
509　7), thus resulting in significant decreases in the GHG emission intensity (emissions per unit

510 product) of rice.

511   In terms of total annual CH_4 emissions from paddy fields under traditional water and

512 fertilizer management practices, DNDC simulated an annual mean value of 7892 Gg (1 Gg =

513 10^9 g) C per year over 1981-2010. A nationwide switching from the traditional practice to the

514 comprehensive mitigation measure reduced CH_4 emissions by 1940 Gg C, or 25% in total,

515 and by 8% to 35% across most paddy grid-cells, as shown in Figure 7a. The reduction effect

516 was highly significant in the north part of Jiangxi province, large parts of Hunan and

517 Zhejiang provinces and the south part of Anhui province.

518   In terms of total annual N_2O emissions under traditional management practices, DNDC

519 simulated an annual mean value of 44 Gg N per year over 1981-2010. The nationwide switch

520 of water and management practice from TM to CM reduced N_2O emissions by 17 Gg N or 38%

521 in total, and by 10% to 75% across most paddy grid-cells as shown in Figure 7b. The most

522 significant mitigation effect was simulated in Northeast China, Jiangsu and Ningxia

523 provinces, while there no significant changes in emissions were simulated in Hubei province.

524

525 **4 DISCUSSION AND CONCLUSION**

526   Our site simulations suggest that comprehensive mitigation measures that combine

527 midseason drainage and balanced fertilizer applications can significantly reduce CH_4 and

528 N_2O emissions from paddy rice fields, without rice yield losses. This result is in line with

529 field experiment results from the Nanjing station presented by Cai et al. (1997). Our site

530 simulations for obtaining a balanced N fertilizer application ratio highlighted a 25%

531 excessive application rate in Zhenjiang station of Jiangsu province, very close to the 23.6%

532 estimate that resulted from the field experiments of Chen et al. (2016) and the 15-25%

533 estimate made by Hofmeier et al. (2015) in the same province.

534   Our aggregated results across all paddy fields in China show that mean annual total CH_4

535 emissions under prevalent traditional management practices is 7892 Gg C yr^{-1} over the period

536 of 1981-2010, well within the range of 6000 to 12000 Gg C yr^{-1} simulated by Li et al. (2005)

537 based on DNDC runs using county-level data, but still about double the levels estimated

538 under the IPCC Tier 1 methodology by FAOSTAT (FAOSTAT, 2016). In terms of average

539 CH_4 fluxes per hectare under traditional management practices, our result is 186 kg C ha^{-1} yr^{-}

540 ^{1} for the period of 1981-2010, which is in the interval of 9 to 725 kg C ha^{-1} yr^{-1} indicated by a

541 field validation of the DNDC model in Cai et al. (2003) and the interval of 90 to 214 kg C ha^{-}

542 ^{1} yr^{-1} produced by DNDC simulations at two sites in Liaoning and Jiangsu Provinces

543 (Frolking et al., 2004). Our results also show that the annual total N_2O emission from paddy

544 fields under traditional management practices is 43.9 Gg N yr^{-1}, which is close to the result of

545 35.7 Gg N as calculated for China's paddy fields as a whole by Gao et al. (2011), but

546 significantly lower than the simulation results of 290 to 410 Gg N yr^{-1} as presented in Li et al.

547 (2005). In terms of average N_2O fluxes per hectare per year under the traditional management

548 practice, our result is 1.04 kg N ha^{-1} yr^{-1} during 1981-2010, which is located in the interval of

549 0.14 to 4.42 kg N ha^{-1} yr^{-1} as reported in Akiyama et al. (2005) based on the a summary of the

550 observed data.

551   The contribution of this research is not limited to confirming the existing assessments on

552 CH_4 and N_2O inventories. It aims to quantify, at both the site and regional levels, the extent to

553 which the major alternative water and fertilizer management methods can lead to significant

554 reduction of CH_4 and N_2O emissions without causing yield reduction. For this purpose, this

555 research enriches the value set of cultivar parameters of the DNDC model by effectively

556 communicating with the DSSAT-rice model and the AEZ model, and up-scales the DNDC

557 runs within each of the AEZ rice cropping zones.

558   More importantly, our systematic assessment focused on the effect of comprehensive

559 mitigation measures, which combines a balanced fertilizer application approach with the

560 midseason field drying method, and their evaluation against corresponding impacts on food

561 production potential. Our results show that switching from traditional fertilizer and water

562 management practices to comprehensive mitigation measures can lead to significant

563 reductions in both CH_4 and N_2O emissions. CH_4 emission can be reduced by 18-40% across

564 the nine representative stations, by 8-35% across almost all paddy grid-cells of China, and by

565 25% at the national level. N_2O emission can be reduced by 12-60% across the nine

566 representative sites, by 10-75% across a vast majority of grid-cells in China's paddy fields,

567 and by 38% at the national level. These findings indicate that there is significant room for

568 reducing GHG emissions in the Chinese rice producing sector. Measures such as midseason

569 drainage and balanced fertilization, based on crop requirements and soil testing, can achieve

570 the triple benefits of maintaining or even in some cases increasing production, while lowering

571 agricultural input costs and reducing GHG emissions. In future research, more mitigation

572 management methods, such as alternate wetting and drying water management for rice

573 (AWD), and returning straw and zero tillage, could be evaluated at both site and regional

574 scale, providing the necessary observation records become available for model calibration.

575   Several limitations characterize this study, some of them generically applicable to all

576 similar modeling exercises involving up-scaling in space from experimental field station

577 results. These include uncertainty in many of the assumptions used to distribute local weather,

soil and management parameters information over grid-cells. Two limitations are specific to this study of paddy rice in China. First, only the most important single rice rotation was considered, while double cropping rice was not studied. This may lead to biased estimation because single cropping system typically require less N fertilizer, with weaker soil denitrification reactions in cases where there is no additional crop and fertilizer inputs in the fallow season. Future studies should investigate GHG emissions dynamics in double rice cropping systems and other rotations with rice. Second, although the nine stations we chose are representative at the two-digit cropping zone level, cultivar differences are present even within individual two-digit cropping zones. The methodology presented in this research will nonetheless be applicable to introduce more local rice cultivars into the DNDC model.

References

589 Abdalla, M., Kumar, S., Jones, M., Burke, J., Williams, M., 2011. Testing DNDC model for simulating soil respiration and assessing the effects of climate change on the CO_2 gas flux from Irish agriculture. Global Planet. Change 78, 106–115.

593 Akiyama, H., Yagi, K., Yan, X., 2005. Direct N2O emissions from rice paddy fields: summary of available data. Global Biogeochem. Cycles 19, GB1005.

595 Alley, R.B., Marotzke, J., Nordhaus, W.D., Overpeck, J.T., Peteet, D.M., Pielke, R.A., et al., 2003. Abrupt Climate Change. Science 299, 2005-2010.

597 Batjes, N. H., 2009. Harmonized soil profile data for applications at global and continental scales: updates to the WISE database. Soil Use Manage. 25, 124-127.

599 Beheydt, D., Boeckx, P., Sleutel, S., Li, C., van Cleemput, O., 2007. Validation of DNDC for 22 long-term N_2O field emission measurements. Atmos. Environ. 41, 6196-6211.

601 Beven, K., Freer, J., 2001. Equifinality, data assimilation, and uncertainty estimation in mechanistic modelling of complex environmental systems using the GLUE methodology. J. Hydrol. 249, 11-29.

604 Blasone, R.S., Vrugt, J.A., Madsen, H., et al. 2008. Generalized likelihood uncertainty estimation (GLUE) using adaptive Markov chain Monte Carlo sampling. Adv Water Resour 31(4): 630-648.

606 Cai, Z., Xing, G., Yan, X., Xu, H., Tsuruta, H., Yagi, K., Minami K., 1997. Methane and nitrous oxide emissions from rice paddy fields as affected by nitrogen fertilizers and water management. Plant Soil 196, 7-14.

609 Cai, Z., Sawamoto, T., Li, C., Kang, G., Boonjawat, J., Mosier, A., et al., 2003. Field validation of the DNDC model for greenhouse gas emissions in East Asian cropping systems. Global Biogeochem. Cycles 17 GB1107.

612 Challinor, A. J., Watson, J., Lobell, D. B., Howden, S. M., Smith, D. R., Chhetri. N. 2014. A meta-analysis of crop yield under climate change and adaptation. Nature Clim. Change 4:287-291. DOI: 10.1038/nclimate2153.

615 Chen, H., Yu, C., Li, C., Xin, Q., Huang, X., Zhang, J., et al., 2016. Modeling the impacts of water and fertilizer management on the ecosystem service of rice rotated cropping systems in China. Agric. Ecosyst. Environ. 219, 49-57.

618 Dong, H., Yao, Z., Zheng, X., Mei, B., Xie, B., Wang, R., et al., 2011. Effect of ammonium-based, non-sulfate fertilizers on CH_4 emissions from a paddy field with a typical Chinese water management regime. Atmos. Environ. 45, 1095-1101.

621 FAO, 2007. Mapping Biophysical Factors That Influence Agricultural Production and Rural Vulnerability. Environment and Natural Resources Series 10. FAO, Rome, Italy.

623 FAO, 2016. Rice Market Monitor, April 2016. Trade and Markets Division, Food and Agriculture Organization of the United Nations, Rome. Available at http://www.fao.org/fileadmin/templates/est/COMM_MARKETS_MONITORING/Rice/Images/

626 RMM/RMM_APR16.pdf.

627 FAO/IIASA/ISRIC/ISSCAS/JRC, 2009. Harmonized World Soil Database (version 1.1). FAO, Rome,
628   Italy and IIASA, Laxenburg, Austria.

629 FAOSTAT, 2016. Emissions-Agriculture Domain. http://www.fao.org/faostat/en/#data/GR/visualize

630 Fischer, G., Nachtergaele, F., Prieler, S., Teixeira, E., van Velthuizen, H.T., Tóth, G., et al., 2012.
631   Global Agro-Ecological Zones (GAEZ v3.0): Model Documentation. IIASA and FAO,
632   Laxenburg, Austria and Rome, Italy.

633 Fischer, G., Shah, M., Tubiello, F.N., van Velthuizen, H.T., 2005. Socioeconomic andclimate change
634   impacts on agriculture: an integrated assessment, 1990–2080.Philosophical Transactions of the
635   Royal Society B 360, 2067–2073.

636 Frolking, S., Li, C., Braswell, R., Fuglestvedt, J., 2004, Short- and long-term greenhouse gas and
637   radiative forcing impacts of changing water management in Asian rice paddies. Glob. Chang. Bio.
638   10, 1180-1196.

639 Fumoto, F., Kobayashi, K., Li, C., Yagi, K., and Hasegawa, T., 2008. Revising a process-based
640   biogeochemistry model (DNDC) to simulate methane emission from rice paddy fields under
641   various residue management and fertilizer regimes. Glob. Change Biol. 14, 382-402.

642 Gao, B., X. T. Ju, Q. Zhang, P. Christie, F. S. Zhang, 2011. New estimates of direct N2O emissions
643   from Chinese croplands from 1980 to 2007 using localized emission factors. Biogeosciences, 8,
644   3011–3024.

645 Gao, M.F., Qiu, J.J., Li, C.S., Wang, L.G., Li, H., Gao, C.L., 2014. Modeling nitrogen loading from a
646   watershed consisting of cropland and livestock farms in China using Manure-DNDC. Agr.
647   Ecosyst. Environ. 185, 88–98.

648 Gijsman, A.J., Jagtap, S.S., Jones, J.W., 2002. Wading through a swamp of complete confusion: how
649   to choose a method for estimating soil water retention parameters for crop models. European
650   Journal of Agronomy 18, 75–105.

651 Gijsman, A.J., Thornton, P.K., Hoogenboom, G., 2007. Using the WISE database to parameterize soil
652   inputs for crop simulation models. Computers and Electronics in Agriculture 56, 85–100.

653 Gilhespy, S.L., Anthony, S., Cardenas, L., Chadwick, D., Pardo A., Li, C., et al., 2014. First 20 years
654   of DNDC (DeNitrification DeComposition): Model evolution. Ecol. Model. 292, 51-62.

655 Giltrap, D., Li, C., Saggar, S., 2010. DNDC: A process-based model of greenhouse gas fluxes from
656   agricultural soils. Agr. Ecosyst. Enviro. 136, 292-300.

657 Gohari, A., Eslamian, S., Abedi-Koupaei, J., Bavani, A.M., Wang, D., Madani, K., 2013.Climate
658   change impacts on crop production in Iran's Zayandeh-Rud River Basin.Science of the Total
659   Environment 442, 405–419.

660 He, J., Jones, J., Graham, W., Dukes, M., 2010. Influence of likelihood function choice for estimating
661   crop model parameters using the generalized likelihood uncertainty estimation method. Agr. Syst.
662   103, 256-264.

663   Hofmeier, M., Roelcke, M., Han, Y., Lan, T., Bergmann, H., Böhm, D., et al., 2015. Nitrogen

664   management in a rice-wheat system in the Taihu Region: recommendations based on field

665   experiments and surveys. Agric. Ecosyst. Environ. 209, 60-73.

666   Hoogenboom G, Jones JW, Wilkens PW, et al. 2010. Decision Support System for Agro-technology

667   Transfer, Version 4.5, Volume 1: Overview. University of Hawaii, Honolulu, USA.

668   IPCC, 2006. IPCC Guidelines for National Greenhouse Gas Inventories, Inst. for Global Environ.

669   Strategies, Hayama, Japan.

670   IPCC, 2013. Climate Change 2013: The Physical Science Basis. Contribution of Working Group I to

671   the Fourth Assessment Report of the Intergovernmental Panel on Climate Change. Cambridge

672   Univ. Press. Cambridge.

673   IPCC, 2014. Climate Change 2014: Summary for Policymakers. Contribution of Working Group III to

674   the Fourth Assessment Report of the Intergovernmental Panel on Climate Change. Cambridge

675   Univ. Press. Cambridge.

676   Itoh, M., Sudo, S., Mori, S., Saito, H., Yoshida, T., Shiratori, Y., et al., 2011. Mitigation of methane

677   emissions from paddy fields by prolonging midseason drainage. Agric. Ecosyst. Environ. 141,

678   359-372.

679   Johnson-Beebout, E. S., Angeles, R. O., Alberto, R. M. C., Buresh, J. R., 2009. Simultaneous

680   minimization of nitrous oxide and methane emission from rice paddy soils is improbable due to

681   redox potential changes with depth in a greenhouse experiment without plants. Geoderma. 149,

682   45-53.

683   Jones, W. J., Antle, M. J., Basso, B., Boote, J. K., Conant, T. R., Foster, I., et al., 2016. Brief history of

684   agricultural systems modeling. Agr Syst. http://dx.doi.org/10.1016/j.agsy.2016.05.014）

685   Jones, J.W., Hoogenboom, G., Porter, C.H., Boote, K.J., Batchelor, W.D., Hunt, L.A., et al., 2003. The

686   DSSAT cropping system model. Europ. J. Agronomy 18, 235-265.

687   Karl, T.R., Trenberth, K.E., 2003. Modern Global Climate Change. Science 302, 1719-1723.

688   Lane, L. J., 1982. Distributed model for small semi-arid watersheds. 3. Hydr. Div. Am. Soc. Civ. Eng.

689   108, 1114-1131.

690   Li, C., 2000. Modeling trace gas emissions from agricultural ecosystems. Nutr. Cycl. Agroecosys. 58,

691   259-276.

692   Li, C., 2007. Quantifying greenhouse gas emissions from soils: scientific basis and modeling

693   approach. Soil Sci. Plant Nutr. 53, 344-352.

694   Li, C., Frolking, S., Harriss, R., 1994. Modeling carbon biogeochemistry in agricultural soils. Global

695   Biogeochem. Cycles 8, 237-254.

696   Li, C., Frolking, S., Frolking, T.A., 1992. A model of N_2O evolution from soil driven by rainfall

697   events: 1. Model structure and sensitivity. J. Geophys. Res. 97, 9759-9776.

698   Li, C., Frolking, S., Xiao, X., Moore, B., Boles, S., Qiu, J., et al., 2005. Modeling impacts of farming

699   management alternatives on CO_2, CH_4, and N_2O emissions: A case study for water management

700   of rice agriculture of China. Global Biogeochem. Cycles 19, GB3010.

701 Li, C., Salas, W., Zhang, R., Krauter, C., Rotz, A., and Mitloehner, F., 2012. Manure-DNDC: a

702   biogeochemical process model for quantifying greenhouse gas and ammonia emissions from

703   livestock manure systems. Nutr. Cycl. Agroecos. 93, 163-200, doi: 10.1007/s10705-012-9507-z,

704   2012.

705 Liu, J., Liu, M., Tian, H., Zhuang, D., Zhang, Z., Zhang, W., et al., 2005. Spatial and temporal patterns

706   of China's cropland during 1990–2000: an analysis based on Landsat TM data. Remote Sensing

707   of Environment 98, 442–456.

708 Masutomi, Y., Takahashi, K., Harasawa, H., Matsuoka, Y., 2009. Impact assessmentof climate change

709   on rice production in Asia in comprehensive considerationof process/parameter uncertainty in

710   general circulation models. Agriculture,Ecosystems and Environment 131, 281–291.

711 McCuen, R.H., 2003. Modeling Hydrologic Change: Statistical Methods. Lewis Publishers, New York.

712 Miao, Y., Stewart, B.A., Zhang, F., 2010. Long-term experiments for sustainable nutrient management

713   in China. A review. Agron. Sustain. Dev. 31, 397-414.

714 Pathak, H., Li, C., Wassmann, R., 2005. Greenhouse gas emissions from Indian rice fields: calibration

715   and upscaling using the DNDC model. Biogeosciences 2, 113-123.

716 Penning de Vries, F., Teng, P., Metselaar, K., Hunt, L.A., 1992. Designing Improved Plant Types: A

717   Breeder's Viewpoint, Systems Approaches for Agricultural Development, vol. 2. Springer,

718   Netherlands, pp. 3–17.

719 Pohlert, T., 2004. Use of empirical global radiation models for maize growth simulation. Agricultural

720   and Forest Meteorology 126, 47–58.

721 Prasada Rao, G.S.L.H.V. 2008. Agricultural Meteorology, PHI Learning Pvt. Ltd., Delhi.

722 Ritchie, J.T., Godwin, D.C., Singh, U., 1989. Soil and Water inputs for IBSNAT crop models, In

723   DSSAT, IBSNAT Symposium, Part I, Las Vegas, Nevada.

724 Seidl, M., Batchelor, W., Fallick, J., Paz, J., 2001. GIS-crop model based decision support system to

725   evaluate corn and soybean prescriptions. Appl. Eng. Agric. 17, 721-728.

726 Smith, P., Trines, E., 2007. Agricultural measures for mitigating climate change: will the barriers

727   prevent any benefits to developing countries? Int. J. Agric. Sust. 4, 173-175.

728 Smith, P., 2012. Agricultural greenhouse gas mitigation potential globally, in Europe and in the UK:

729   what have we learnt in the last 20 years? Glob. Chang. Biol. 18, 35-43.

730 Tang, H.J., Qiu, J.J., Van Ranst, E., Li, C.S. 2006. Estimations of soil organic carbon storage in

731   cropland of China based on DNDC model. Geoderma 134, 200–206.

732 Thorp, K., DeJonge, K., Kaleita, A., Batchelor, W., Paz, J., 2008. Methodology for the use of DSSAT

733   models for precision agriculture decision support. Comput. Electron. Agr. 64, 276-285.

734 Tian, Z., Zhong, H., Shi R., Sun, L., Fischer, G., Liang, Z., 2012. Estimating potential yield of wheat

735   production in China based on cross-scale data-model fusion. Front Earth Sci. 6, 364-372.

22

736 Tian, Z., Zhong, H., Sun, L., Fischer, G., van Velthuizen, H., Liang, Z. 2014. Improving performance
737   of Agro-Ecological Zone (AEZ) modeling by cross-scale model coupling: An application to
738   japonica riceproduction in Northeast China. Ecological Modelling 290, 155–164.

739 Tonitto, C., David, M.B., Drinkwater, L.E., Li, C.S., 2007. Application of the DNDC model to tile-
740   drained Illinois agroecosystems: model calibration, validation, and uncertainty analysis. Nutr.
741   Cycl. Agroecosys. 78, 51–63.

742 Tubiello, F.N., Fischer, G., 2007. Reducing climate change impacts on agriculture:global and regional
743   effects of mitigation, 2000–2080. Technological Forecastingand Social Change 74, 1030–1056.

744 Verburg, P.H., Chen, Y., Veldkamp, T., 2000. Spatial explorations of land use change and grain
745   production in China. Agric. Ecosyst. Environ. 82, 333-354.

746 Wang, G., Chen, S. 2012. A review on parameterization and uncertainty in modeling greenhouse gas
747   emissions from soil. Geoderma 170, 206–216.

748 Wang, L.G., Qiu, J.J., Tang, H.J., Li, H., Li, C.S., van Ranst, E. 2008. Modelling soil organic carbon
749   dynamics in the major agricultural regions of China. Geoderma 147, 47–55.

750 Wang, S., Huang, G.H., Huang, W., et al. 2015. A fractional factorial probabilistic collocation method
751   for uncertainty propagation of hydrologic model parameters in a reduced dimensional space. J
752   Hydrol 529: 1129–1146.

753 Wu, F., Zhang, H., Li, L., Chen, F., Huang, F., Xiao, X., 2008. Characteristics of CH_4 emission and
754   greenhouse effects in double paddy soil with conservation tillage. Scientia Agricultura Sinica 41,
755   2703-2709.

756 Yan, X., Akiyama, H., Yagi, K., Akimoto, H., 2009. Global estimations of the inventory and
757   mitigation potential of methane emissions from rice cultivation conducted using the 2006
758   Intergovernmental Panel on Climate Change Guidelines. Global Biogeochem. Cycles 23,
759   GB2002.

760 Zhang, L., Zhuang, Q., Li, X., Zhao, Q., Yu, D., Liu, Y., et al. 2016. Carbon sequestration in the
761   uplands of Eastern China: An analysis with high-resolution model simulations. Soil & Tillage
762   Research 158, 165–176.

763 Zhang, Y., Li, C., Trettin, C. C., Li, H., and Sun, G., 2002. An integrated model of soil, hydrology and
764   vegetation for carbon dynamics in wetland ecosystems, Global Biogeochem. Cy. 16, 1061, doi:
765   10.1029/2001GB001838.

766

767

768   Table 1. Information of the nine representative observation stations

Site	Location	Soil texture	Mean daily temperature range (°C)	Precipitation range (mm)	Mean precipitation (mm)
AHHF	31.87°N 117.23°E	Loam	24.2-27.3	228.4-1064.2	578.6
HNXY	32.12°N 114.08°E	Silty-clay	24.2-27	151.7-1161.4	677.0
JLYJ	42.88°N 129.47°E	Clay-loam	15.2-18.4	331.7-790.0	467.4
JSZJ	32.18°N 119.47°E	Clay-loam	25-27.1	269.8-1327.0	669.1
JXNC	28.55°N 115.95°E	Clay-loam	23-25.6	501.4-1341.2	820.2
LNTT	41.42°N 123.32°E	Sandy-clay-loam	19-22.3	354.1-916.3	569.5
SCCD	30.7°N 103.83°E	Clay-loam	22-24.1	488.1-1050.2	733.8
SDLY	35.05°N 118.35°E	Clay-loam	22.5-24.9	441.8-1106.7	715.6
GDGZ	23.05°N 113.47°E	Clay-loam	18.9-25.8	570.1-1640.7	1012.5

769   Notes: The statistics on temperature and precipitation is for the single rice growing season over the period of

770   1981-2010.

771

772

773

774

775   Table 2. Observed level of fertilizer application and the balanced fertilizer ratio (BFR) at the

776   nine stations

Site	AHHF	HNXY	JLYJ	JSZJ	JXNC	LNTT	SCCD	SDLY	GDGZ
Fertilizer App (kgN ha^{-1})	335.0	255.3	330.5	273.0	334.5	203.6	252.9	186.0	250.0
BFR-1 (%)	85	80	65	75	90	80	95	70	65
BFR-2 (%)	85	80	65	75	80	95	95	70	65

777   Notes: BFR-1 refers to the BFR under continues flooding scenario and BFR-2 under the midseason drainage and

778   comprehensive management scenarios.

779

780

781

782

783   Table 3. Calibrated values of cultivar parameters for DNDC at the nine representative sites

Site	GB	HI	GF	LF	SF	RF	ND	OT	TDD
AHHF	11436.33	0.5273	0.448	0.201	0.201	0.15	209.588	27	3859.00
HNXY	11597.39	0.5179	0.440	0.205	0.205	0.15	215.382	25	3776.00
JLYJ	10761.25	0.5311	0.452	0.199	0.199	0.15	168.919	22	2965.00
JSZJ	11539.50	0.5078	0.432	0.209	0.209	0.15	217.479	25	3884.30
JXNC	9055.58	0.6058	0.514	0.168	0.168	0.15	150.094	30	2594.95
SCCD	9883.21	0.5644	0.480	0.185	0.185	0.15	172.349	25	3873.80
SDLY	9900.00	0.4958	0.422	0.214	0.214	0.15	158.480	25	3808.60
LNTT	9528.57	0.5521	0.470	0.190	0.190	0.15	146.662	22	3471.55
GDGZ	7801.40	0.5486	0.466	0.192	0.192	0.15	138.883	30	3351.45

784   Notes: GB denotes grain biomass (kg/ha/yr), HI harvest index, GF grain-fraction, LF leaf-fraction, SF stem-
785   fraction, RF root-fraction, ND N demand (kgN/ha/yr), OT optimum temperature (°C), TDD accumulative
786   degree days from emergence to maturity (°C).

787

788

789

790

791   Table 4. The observed best attainable yield, the minimum, mean, and maximum of the
792   simulated yields, and the average RAE at the nine stations (1981-2010)

Site	Observed yield (kg)	Simulated attainable yield (kg)			Average RAE (%)
		Minimum	mean	maximum	
AHHF	10,815	8,869	10,266	10,952	5.086
HNXY	10,024	9,141	10,125	10,992	0.998
JLYJ	10,500	9,249	10,009	10,381	4.686
JSZJ	10,140	8,891	10,494	10,852	3.491
JXNC	8,812	8,268	8,623	8,892	2.156
SCCD	9,240	8,861	9,240	9,531	0.000
SDLY	8,580	8,893	9,242	9,582	7.716
LNTT	9,184	8,276	8,752	9,195	4.704
GDGZ	6,945	7,235	7,511	7,677	8.135

793

794

795

25

796　Table 5. Rice yield, CH$_4$ and N$_2$O emissions at the Nanjing site in 1994.

	Observed (Cai et al., 2003)	Simulated with DNDC		
		Our results	*Cai et al. (2003)*	*Fumuto et al. (2008)*
Yield (kg ha^{-1})	6918.8	7782.5		
CH$_4$ (kg C ha^{-1})	57.8	77	47.1	88
N$_2$O (kg N ha^{-1})	0.62	0.5	5.70	

797　Note: Observation records and simulation results are for the same single rice growing season in 1994.

798
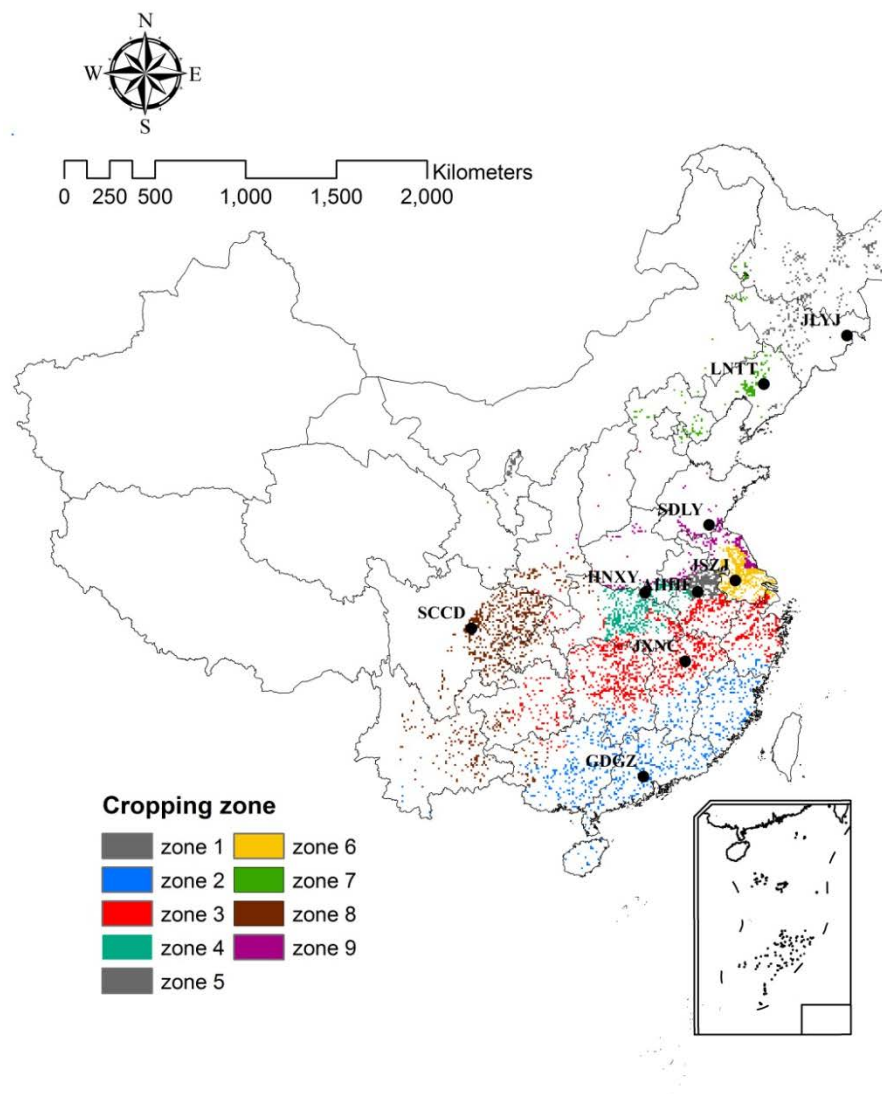
799
800
801 Figure 1. The reclassified rice cropping zone map of China based on 9 observation stations.

802 Color scheme distinguishes the 9 zones and big black dots stand for the observation stations

803
804
805
806
807
808
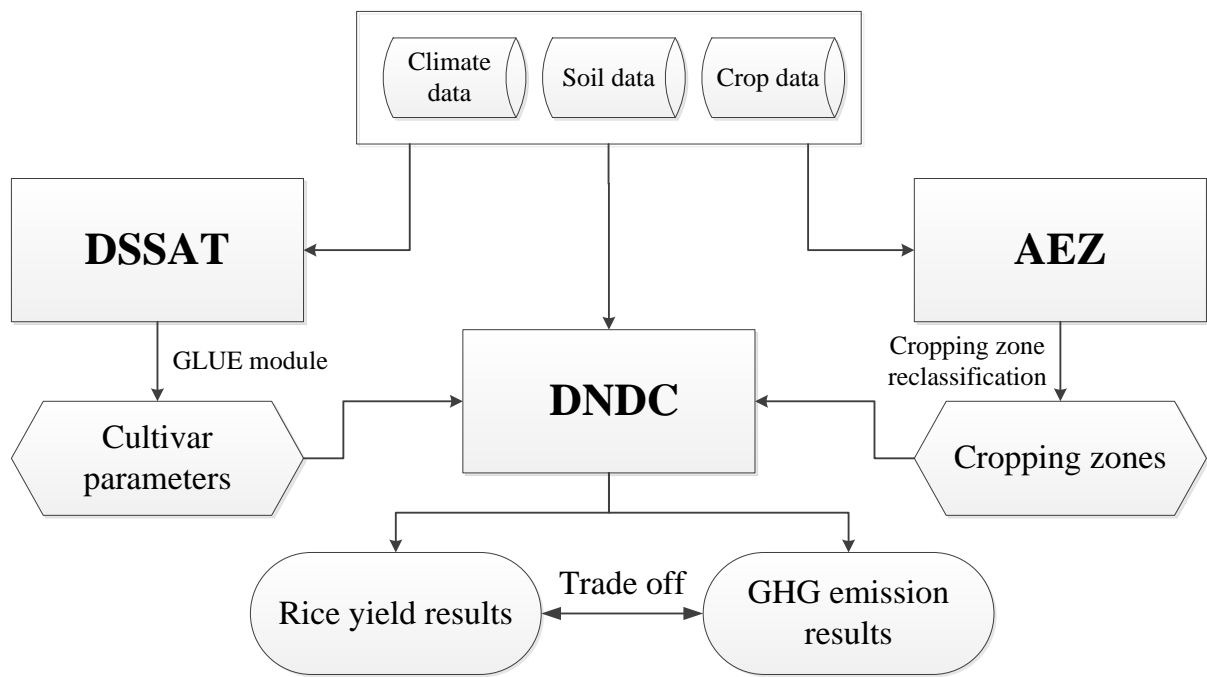
Figure 2. Flowchart of the model coupling procedure

809

810

811

812

813

814

815
816
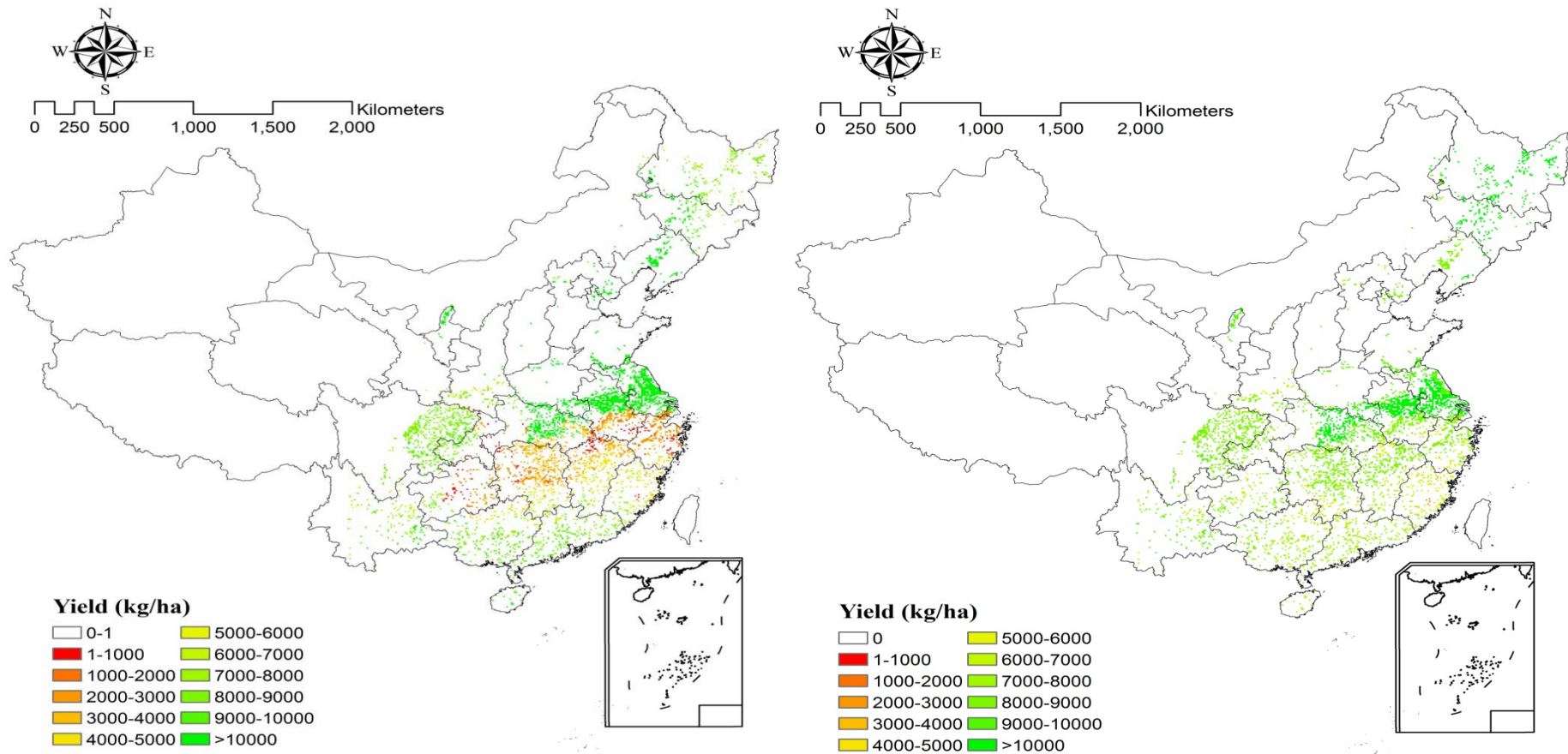
817 Figure 3. The grid-cell results of rice yield simulation from the original DNDC (left, denoted as Figure 3-a) and coupled DNDC (right, Figure 3-
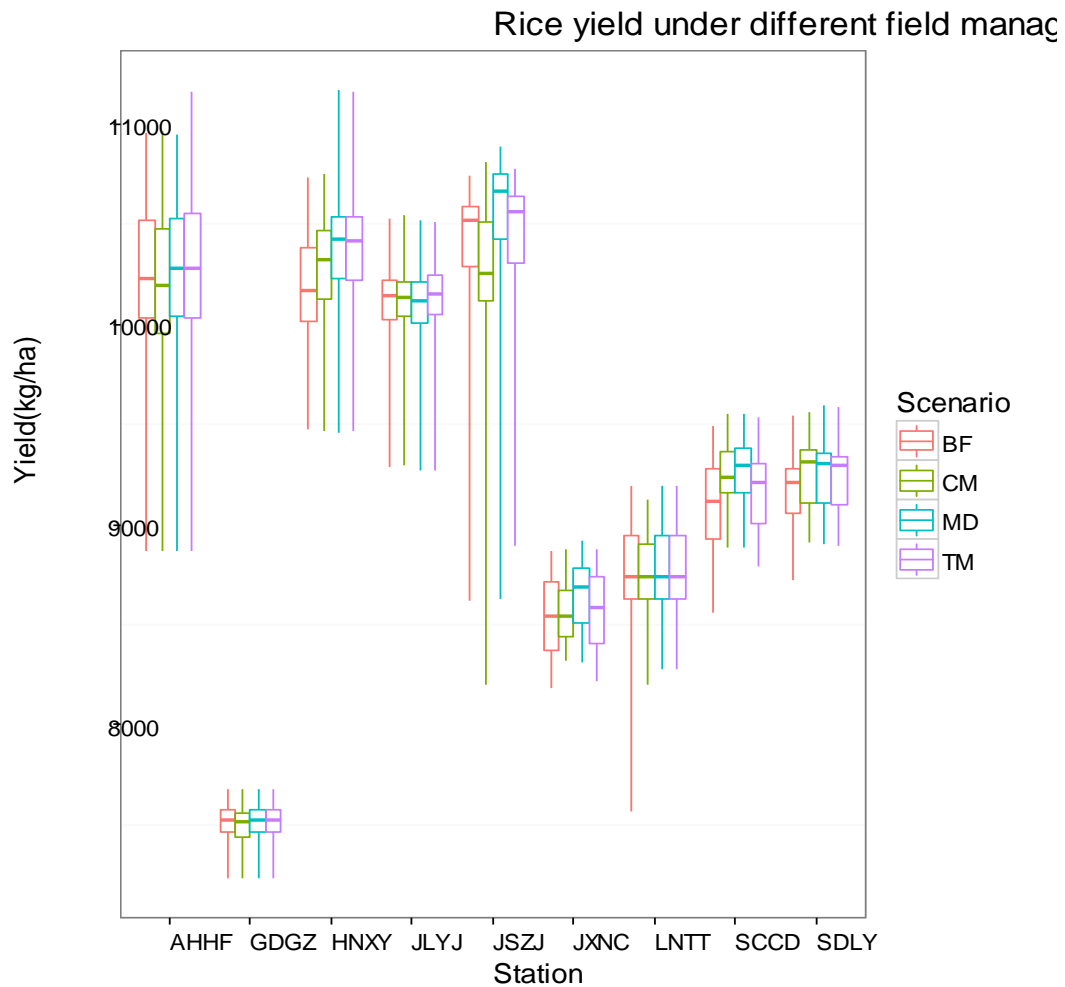
818 b) model, average over 1981-2010

819

820

821

822

823 Figure 4. The boxplots of rice yields under field management scenarios of Traditional

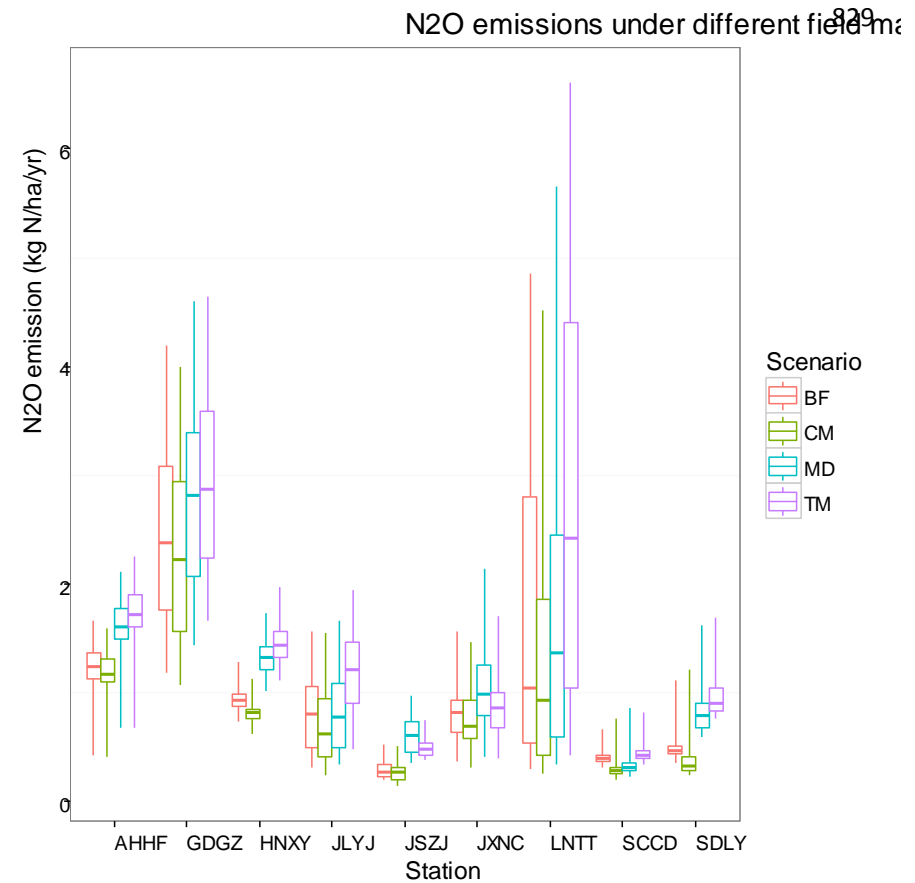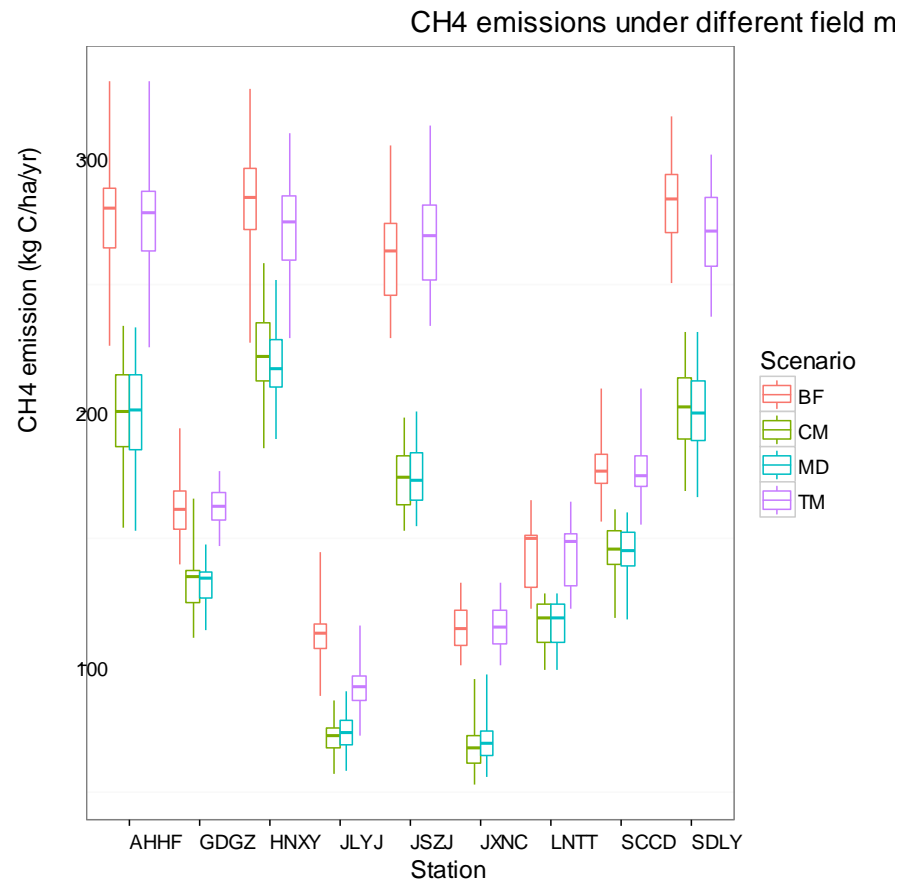824 Management (TM), Balanced Fertilizer (BF), Midseason Drainage (MD) and Comprehensive

825 Management (CM).

826

827

828

829

Figure 5. The boxplots of methane emission (left, denoted as Figure 5-a.) and nitrous oxide emission (right, Figure 5-b.) under field management scenarios of Traditional Management (TM), Balanced Fertilizer (BF), Midseason Drainage (MD) and Comprehensive Management (CM).
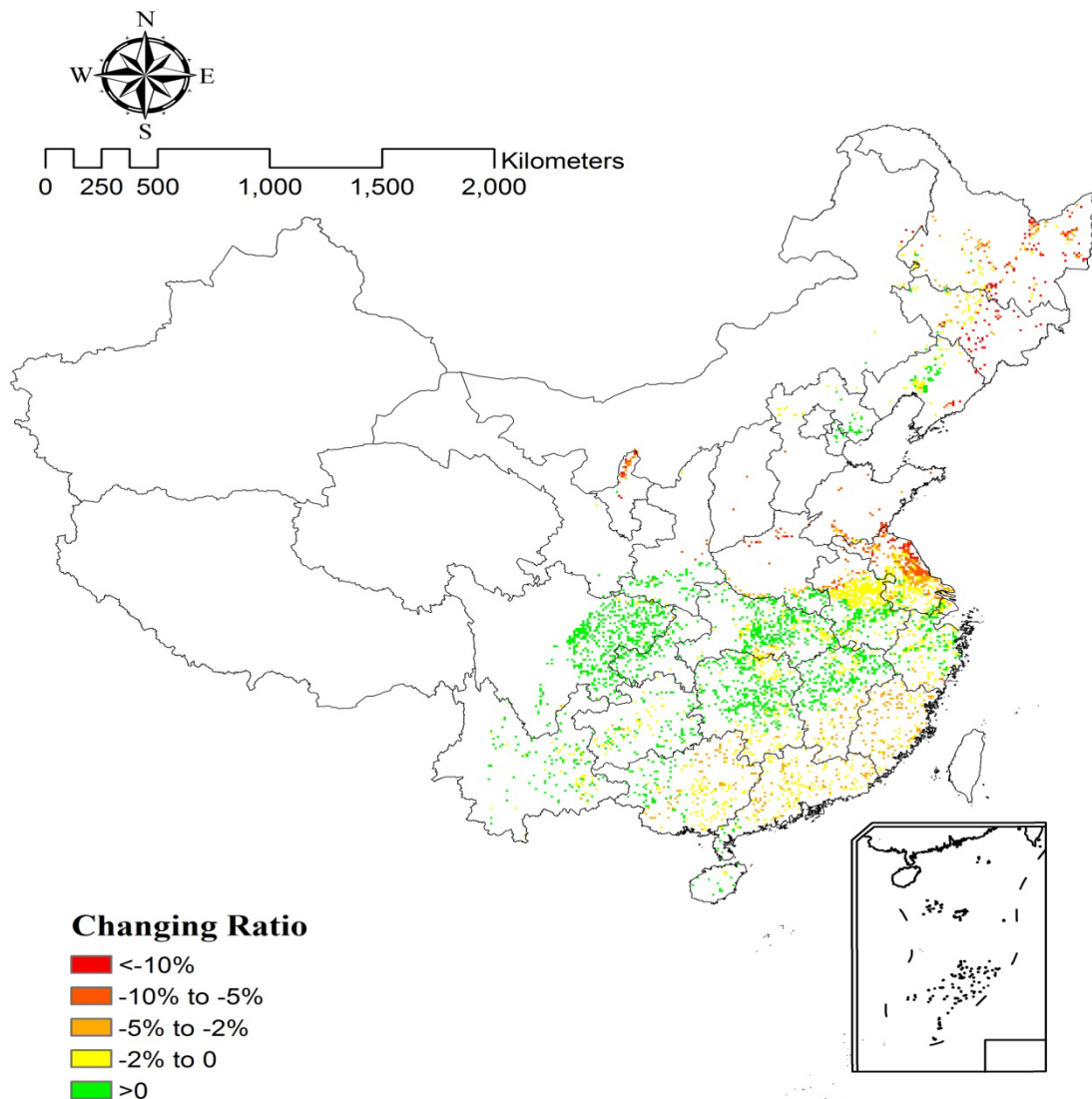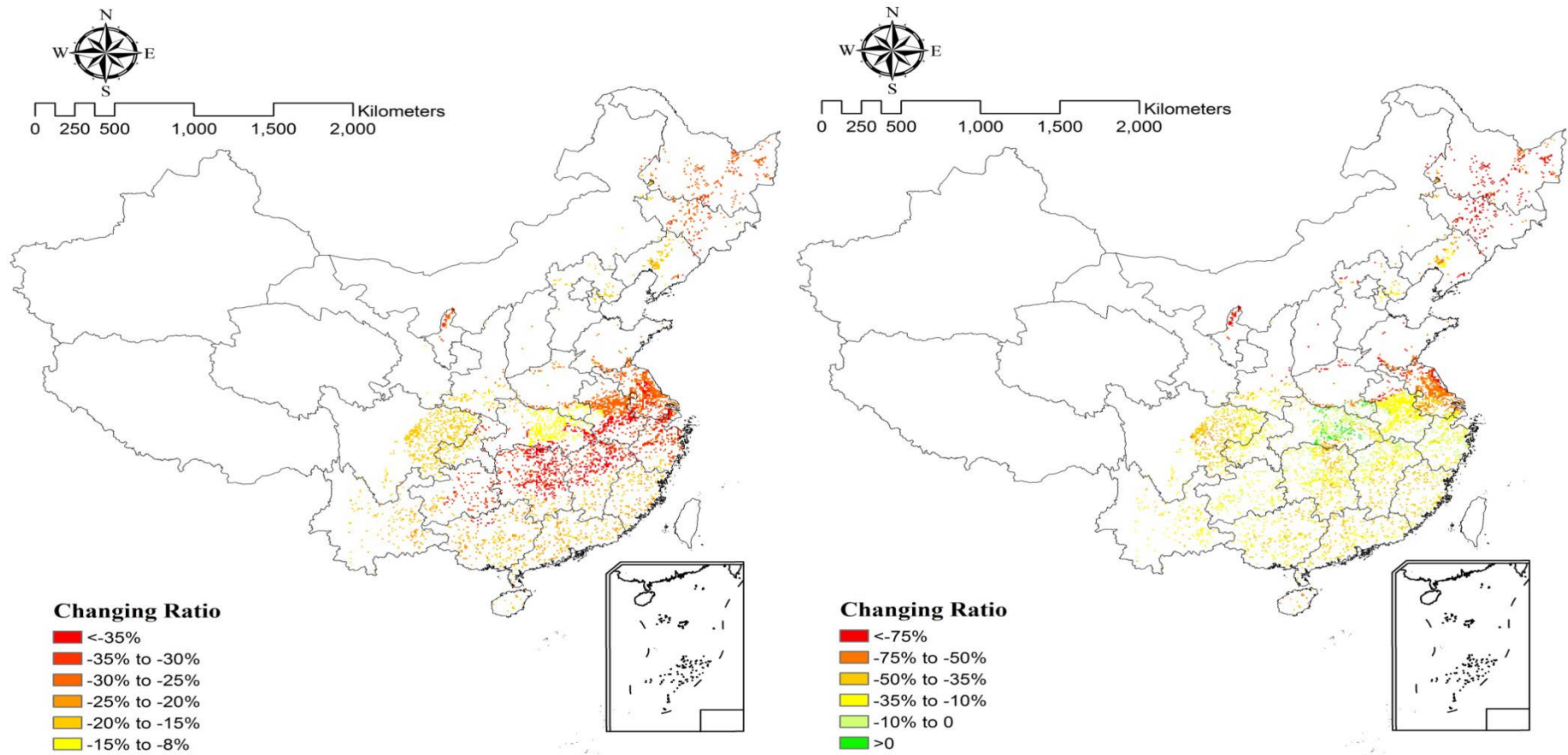
830
831

832

833

834

835 Figure 6. Changes of the simulated best attainable yields at the grid-cell level under the

836 comprehensive mitigation scenario versus the traditional management scenario

837

Figure 7. Changes in CH_4 emission (left, denoted as Figure 7-a.) and N_2O emission (right, Figure 7-b.) at the grid-cell level under the comprehensive mitigation scenario versus traditional management scenario